International Journal of Greenhouse Gas Control 88 (2019) 311–320

Contents lists available at ScienceDirect

International Journal of Greenhouse Gas Control

journal homepage: www.elsevier.com/locate/ijggc

# Experimental study on comprehensive carbon capture performance of TETA-based nanofluids with surfactants

Yanchi Jiang, Zhongxiao Zhang*, Junjie Fan, Juan Yu, Degui Bi, Boyang Li, Ziqi Zhao, Mengchuan Jia, Aiwei Mu

*School of Mechanical Engineering, Shanghai Jiao Tong University, 800 Dongchuan RD, Minhang District, Shanghai 200240, China*

ARTICLE INFO

*Keywords:*
$CO_2$ capture
Chemical absorption
Nanofluids
Surfactants
Energy consumption

ABSTRACT

Absorbents have become a vital factor in determining the performance of chemical absorption technique for $CO_2$ capture. In recent years, amine-based nanofluids have shown a promising potential to develop high-performance absorbents. Thus, a bubbling reaction system was implemented to comprehensively study the $CO_2$ capture properties of TETA-based nanofluids in this work. Three kinds of nanoparticles and surfactants were adopted to prepare nanofluids. The important parameters, such as ultrasonic vibration time, particle size and surfactants mass fraction, were considered to evaluate the comprehensive $CO_2$ capture performance. It was found that nanofluids shows better $CO_2$ capture performance than blank TETA solutions, which is mainly due to the enhancement of liquid-phase turbulence and the microscopic motion of nanoparticles. 1.0 h is considered as the most reasonable ultrasonic time for $CO_2$ absorption in this experimentation. There is an optimal $SiO_2$-nanoparticle mass fraction of 0.10 wt.%, the enhancement factors of ab/desorption ($E_{ab}$ and $E_{de}$) can respectively increase up to 1.29 and 1.23. The larger size can reduce the relative particle surface area and energy, 45 nm $SiO_2$-nanofluids show lower energy consumption when the $CO_2$-loading reaches $\alpha_s$. Enhancement factors of both ab/desorption for $TiO_2$ and $SiO_2$ are very close and evidently higher than $Al_2O_3$ due to the nanoparticles' different $CO_2$ adsorption performance. The addition of surfactant C-Na can effectively promote the mass transfer performance of nanofluids, but Triton X-100 and SDBS will cause inhibition effect when mass fraction exceeds 0.01 wt.%.

## 1. Introduction

Climate change has become a major concern of the government and public. The concentration growth of greenhouse gases (77% $CO_2$) generated by population and economy development is the main causes of global warming, and the carbon emission issue is becoming increasingly acute (Liu and Gallagher, 2010). Meanwhile, China has now become the largest carbon emission country of the world (Kong et al., 2016). The energy structure of "rich in coal, but not oil and gas" cannot change in the short term. Thus, how to reduce carbon emission from coal utilization proves to be the vital subject that determines the sustainability of coal-fired power industry (Wang and Liu, 2015).

Carbon capture and storage technology (CCS) provides an effective way to change this dilemma, the technical routes can be mainly divided into post-combustion, pre-combustion and oxy-fuel combustion technologies (Abu-Zahra et al., 2007). Among them, post-combustion is specifically aimed at coal-fired power plants, and will continue to be the mainstream carbon capture technique in the follow-up time. However, the coal-fired power plants with CCS system suffers the resulting efficiency penalty in the process of steam power cycle (Pohlmann et al., 2016). Thus, developing high-efficiency and low-energy-consumption carbon capture technique should be the momentous way to realize near zero-emission (Notz et al., 2012).

Recently, chemical absorption method is gradually maturing in post-combustion process (Jilvero et al., 2012), which is largely contribute to the fast developing of the absorbents' kinetics, thermodynamics and hydrodynamics (Liu et al., 2019a, b; Yuan et al., 2018). The use of traditional amine absorbents, such as monoethanolamine (MEA), restricts its application prospects due to degradation, foaming, energy penalty, and etc. (Fang et al., 2012; Saiwan et al., 2013; Xie et al., 2017). Each energy penalty increase of 1 MJ/kg $CO_2$ will cause 2% decrease of power supply efficiency, the promotion of absorption efficiency can effectively lessen device scale and operating cost (Goto et al., 2013). Therefore, it is crucial to exploit high-performance absorbents with considerable absorption efficiency, impressive $CO_2$-loading and less energy consumption. Compared with traditional

* Corresponding author.
*E-mail address:* zhzhx222@163.com (Z. Zhang).

https://doi.org/10.1016/j.ijggc.2019.06.024
Received 25 October 2018; Received in revised form 15 May 2019; Accepted 25 June 2019
Available online 28 June 2019

**Nomenclature**

| | |
|---|---|
| CCS | Carbon capture and storage |
| TETA | Triethylene-tetramine |
| C-Na | Sodium citrate |
| SDBS | Sodium dodecyl benzene sulfonate |
| $Q_i$ | Inlet gas flow rate, ml/min |
| $Q_o$ | Outlet gas flow rate, ml/min |
| $N_{ab}$ | Absorption rate, ml/min |
| $N_{de}$ | Desorption rate, ml/min |
| $\alpha$ | $CO_2$-loading of absorbents, mol $CO_2$/mol amine |
| $V_1$ | Pre-reaction value of the inflator, ml |
| $V_2$ | Post-reaction value of the inflator, ml |
| $C$ | Solution concentration, mol/L |
| $f$ | Temperature correction coefficient |
| $E_{ab}$ | Absorption enhancement factor |
| $E_{de}$ | Desorption enhancement factor |
| $\alpha_{ab}$ | $CO_2$-loading of nanofluids, mol $CO_2$/mol amine |
| $\alpha_{ab,-b}$ | $CO_2$-loading of blank solution, mol $CO_2$/mol amine |
| $\alpha_{de}$ | $CO_2$-loading of desorption process of nanofluids, mol $CO_2$/mol amine |
| $\alpha_{de,\ eq}$ | $CO_2$-loading of reaction equilibrium state of nanofluids, mol $CO_2$/mol amine |
| $\alpha_{de\text{-}b}$ | Blank solution's $CO_2$-loading in desorption process, mol $CO_2$/mol amine |
| $\alpha_{de,\ eq\text{-}b}$ | Blank solution's $CO_2$-loading of reaction equilibrium state, mol $CO_2$/mol amine |
| $Q_{de}$ | Energy consumption of desorption process, kJ |
| $Q_{re}$ | Relative energy consumption of desorption process, MJ/kg $CO_2$ |
| $q_i$ | Initial and final reading of electric power detector, kJ |
| $q_o$ | Final reading of electric power detector, kJ |
| $\alpha$ | Standard $CO_2$-loading, mol $CO_2$/mol amine |
| $\alpha_i$ | Initial $CO_2$-loading, mol $CO_2$/mol amine |
| $y_{sur}$ | Mass fraction of surfactants, % |

absorbents (MEA and MDEA), Triethylene-tetramine (TETA) has higher boiling point and lower viscosity (Yuan et al., 2018)). Besides that, a TETA molecule has two secondary and primary amino groups (Wang et al., 2013), which makes TETA susceptible to the influence of degradation but possess an appreciable $CO_2$-loading that is much higher than MEA by a unit mass (Kim et al., 2014; Schäffer et al., 2012). Meanwhile, the reaction rate of TETA is proved 2–3 times higher than MDEA (Chen et al., 2011). These studies indicate that TETA has more a preferable $CO_2$ capture performance than some other mainstream absorbers, and it is feasible to develop novel absorbents by TETA-based solution (Kim et al., 2014; Schäffer et al., 2012; Wang et al., 2013).

Moreover, nanofluids have shown potential for developing high performance $CO_2$ capture absorbent (Zhang et al., 2016). Since Choi proposed the concept of nanofluids in 1995 (Choi, 1995), studies have shown blending nanoparticles into absorbents can effectively improve the heat and mass transfer performance of solvents (Lee et al., 2011). Although the mass transfer mechanism still remains some uncertainties, the nanoparticles can indeed promote solution's mass transfer performance by accelerating energy transport, micro perturbation and convection of suspended nanoparticles. (Eastman et al., 1996).

For the preparation of nanofluids, the dispersion property largely influences its $CO_2$ capture performance. At present, the dispersing methods primarily contain physical and chemical approaches. Physical method, such as ultrasonic vibration, improves the dispersibility by heightening the Brownian motion energy in nanofluids. In this way, the van der Waals force between particles weakens and the absorbents' mass transfer performance promotes (Jiang et al., 2014). While the chemical methods choose appropriate dispersing agents to enhance the nanofluids' stability (Kim et al., 2006). In addition, rare studies about nanofluids' properties are concerned with carbon capture. Most are limited to the evaluation of the mass transfer performance for unique absorption process. Some vital indicators, such as $CO_2$ removal efficiency, $CO_2$ loading, and desorption energy, have not been fully studied.

Therefore, it is necessary to develop TETA-based nanofluids and study their $CO_2$ capture properties. On the basis, a bubbling reaction system was implemented to evaluate the absorbents' comprehensive capabilities in this work. Three kinds of nanoparticles and surfactants treated by ultrasonic vibration were adopted to form nanofluids. The important parameters, such as ultrasonic vibration time, nanoparticle sizes, surfactants mass fraction, were considered to determine the characteristics of reaction rate, $CO_2$-loading, energy consumption, etc.

## 2. Theoretical background

### 2.1. Mass transfer model

The absorption of carbon dioxide by nanofluids is a gas-liquid mass transfer process with chemical reaction. A variety of absorption models have been proposed so far. Among them, two-film theory is widely applied to the analysis of heat and mass transfer processes. *Sharma* reported that there is a phase interface between gas-liquid two-phase fluids, which presents a gas-liquid equilibrium without mass transfer resistance (Sharma, 1965). *Sema et al.* proposed that the flow regimes of the interface and liquid phase body are respectively laminar and turbulent, while the diffusion in the retained film is considered as steady-state diffusion (Sema et al., 2012).

### 2.2. Reaction mechanism

Triethylene-tetramine (TETA) is a brown yellow viscous liquid with strong hygroscopicity and alkalinity. A TETA molecule contains four nitrogen atoms, two of which belong to primary amine group, and the other two belong to secondary amine group. Thus, the reaction mechanism of TETA can be described by zwitterionic mechanism (Eqs. (1)-(4)):

Zwitterionic generation:

$$CO_2 + R_1R_2NH \rightleftarrows R_1R_2NH^+COO^- \quad (1)$$

Zwitterionic deprotonation:

$$R_1R_2NH^+COO^- + B \rightleftarrows R_1R_2NH_2^+ + R_1R_2HCOO^- \quad (2)$$

Where $B$ is the alkaline substance in solution, mainly including $R_1R_2NH$, $H_2O$, $OH$-.

Carbamate hydrolysis:

$$RH_3^+ + H_2O \rightleftarrows RNH_2 + H_3O^+ \quad (3)$$

Bicarbonate formation:

$$H_2O + RNHCOO^- \rightleftarrows RNH_2 + HCO_3^- \quad (4)$$

### 2.3. Enhancing mass-transfer of nanofluids

The $CO_2$ ab/desorption process of nanofluids contains complex substances, and along with chemical reaction, turbulent diffusion and convective mass transfer. Thus, it is difficult to study the characteristics of matter and energy change in the liquid interior, current studies are mainly based on the laws summarized from experiments. Mass transfer

mechanisms have been proposed and recognized for analysis. Among them, grazing effect mechanism proposed by Kars is based on the assumption that nanoparticles can enter the liquid boundary layer and transport through it to enhance mass transfer performance (Kars et al., 1979). Mixing of the gas-liquid boundary layer mechanism proposed by Ruthiya suggested that nanoparticles can enhance the turbulence and convective mass transfer at the interface, reduce the thickness of the boundary layer and weaken the mass transfer resistance (Ruthiya et al., 2010). Inhibition of bubble coalescence mechanism held the view that nanoparticles wrapped on the surface of bubbles will hinder the coalescence effect and increase the gas-liquid contact area, thus the mass transfer flux and coefficient can be promoted (Roizard et al., 1999). However, these theories can just partially explain the experimental results about their specific application scopes. In general, the consensus of these theories are that the nanofluids' mass transfer effect is mainly affected by molecule perturbation and channel blocking. Therefore, the $CO_2$ capture characteristics of nanofluids will be discussed from above perspectives in this study.

## 3. Experiment

### 3.1. Experimental materials

In this experiment, the amine absorbent was TETA (Titan High-Tech, China) with the purity of 99.9%.The nanoparticles were $TiO_2$, $AL_2O_3$, $SiO_2$ (McLean Biochemical Technology, China) with purity of 99.9% and particle size from 10 to 70 nm. Surfactants were sodium citrate (C-Na), Triton X-100 and sodium dodecyl benzene sulfonate (SDBS) (McLean Biochemical Technology, China) with purity of 99.9%.Gas cylinders (Keju High-Tech, China), with purity of 99.9% $CO_2$ and $N_2$, respectively, were applied to generate simulated gas.

### 3.2. Nanofluids preparation

Because the nanofluids applied in this experiment are prepared by TETA solution, the physicochemical properties are more complicated than pure water, it is inappropriate to adopt "one-step" method to prepare nanofluids. Thus the "two-step method" was recommended in this work due to its extensive versatility and stability (Moraveji et al., 2013). First of all, the 1 mol/L TETA aqueous solution was prepared as the base fluid, then the nanoparticles with a certain mass were weighed according to the requirement and added into the solution. Eventually, the blended solution was dispersed by ultrasonic crushing, and the concentration of TETA should be detected to prevent the error caused by volatilization of water and organic amine. (Nagy et al., 2007). Thus an ultrasonic cell breaker (Jiangsu Tianling Instrument, China) was applied to provide ultrasonic dispersion for preparing efficient and stable TETA-based nanofluid. The TEM (Tecnai G2 spirit Biotwin, the United States) results of different nanoparticles' morphology are shown in Fig. 1, nanoparticle clusters are well dispersed when the bubbles explode by the ultrasonic cavitation effect. When the amplitude of ultrasonic wave reaches a high value, the average distance between the media becomes greater than the critical molecular distance, which causes liquid-medium fracture and uniform dispersion. In order to quantitatively evaluate the dispersion effect of the nanofluids, a nanoparticle Zeta potential analyzer (Brookhaven, the United States) was applied in this work. The main parameters are shown in Table 1.

**Table 1**
Experimental parameters of nanofluids.

| Items | Values |
|---|---|
| Ultrasonic power | 600 W |
| Probe diameter | 15 mm |
| Ultrasound frequency | 25 + 1 kHz |
| Sample preparation capacity | 500 ml |
| Balance accuracy | 10 g/0.001 g |
| Vibration / intermittent time | 3 /5 s |
| Overall ultrasonic time | 0.5-2 h |

### 3.3. Experimental process

The diagram of $CO_2$ capture experimental system for TETA-based nanofluids is shown in Fig. 2. The experimental system is mainly composed of gas supply system, absorption system, desorption system, analysis system, etc. The $CO_2$ capture process is carried out in a bubble reactor, in which the reaction temperature is controlled by a temperature-controlled magnetic stirrer (Shanghai Yangshen, China ( ± 1% FS)).

During absorption process, the $CO_2/N_2$ gas mixture released from high-pressure cylinders and then accessed into buffer tank before being filtered. After that, the treated gas was introduced into the bubble reactor for $CO_2$ absorption. The gas inlet of the reactor was installed as a sand core nozzle (core diameter type: G1) to enhance the bubbles' uniformity. In addition, three reserved holes were set up on the top of the reactor for controlling temperature, monitoring pH value and sampling solution, respectively. The purged gas was cooled by a condenser pipe, in which the circulating water was provided by a miniature pump (EHEIM, Germany). After dewatered by silica gel desiccant, the exhausted gas entered a soap film flowmeter (Qingdao Jingcheng High-tech, China) and then discharged into atmosphere by an air extractor (Panasonic, Japan). The absorption temperature is kept at 313 K by the water bath, while the solution was sampled at regular intervals by pipette guns (TopPette, China) for $CO_2$-loading analyzing.

Moreover, the desorption experiment was basically carried out in the same laboratory equipment. The temperature of rich solution was heated up to 378 K by an electric heating sleeve (Zhengzhou Changzhegn, China), and a layer of insulation cotton is wrapped around the reactor for heat dissipation reduction. Furthermore, the energy consumption value was counted by an electric power detector (Wenzhou Smart Electronic-Tech, China) in real time. And the thermal parameters were analyzed by a thermal conductivity meter (Hot Disk, TPS 2500, Sweden).The working conditions are described in Table 2.

### 3.4. Evaluation parameters

Absorption rata $N_A$. The absorption rate of the bubbling absorption system can be expressed as Eq. (5):

$$N_{ab} = Q_i - Q_o \tag{5}$$

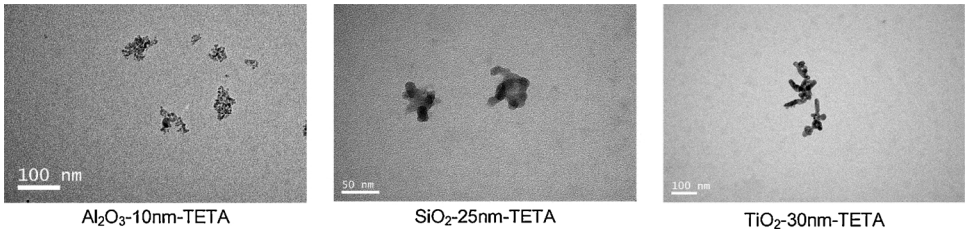


**Fig. 1.** TEM results of different nanoparticles' morphology in TETA solution.

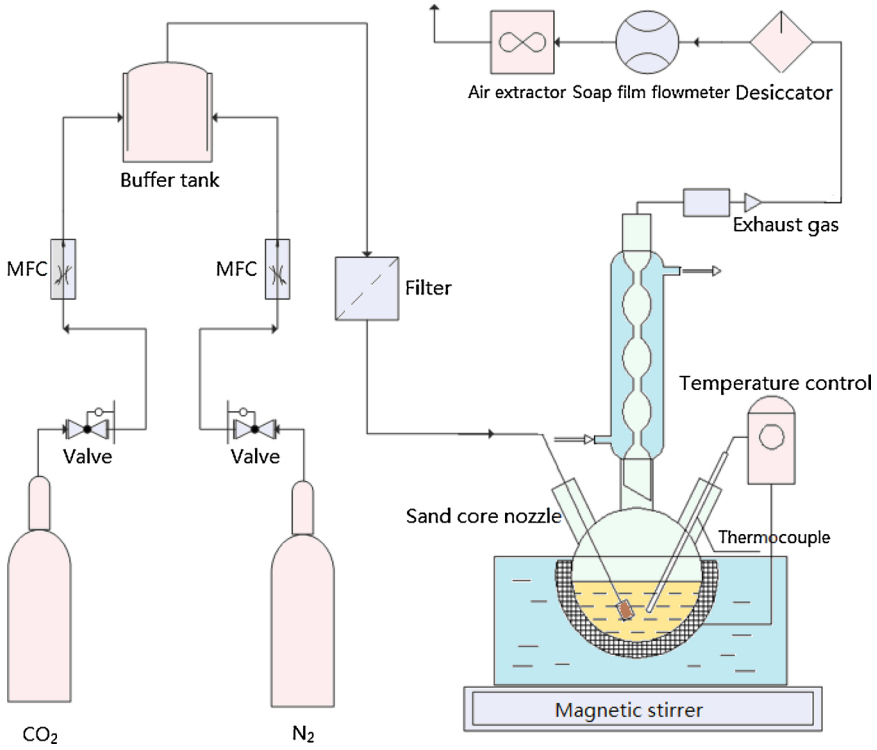


**Fig. 2.** Experimental diagram of bubble reaction system for nanofluids.

**Table 2**
Working conditions of nanofluids $CO_2$ capture performance experiment.

| Subject | Parameters |
|---|---|
| Gas volume flow rate | 1 L/min |
| Absorption temperature | 313 K |
| Desorption temperature | 378 K |
| Absorbent | TETA |
| Absorbent concentration | 0.5-1.5 mol/L |
| Solution volume | 500 mL |
| Nanoparticle types | $TiO_2$, $AL_2O_3$, $SiO_2$ |
| Nanoparticle mass fraction | 0.05- 0.1 wt.% |
| Surfactants | C-Na, SDBS, Triton X-100 |
| Surfactant mass fraction | 0- 0.1 wt.% |

Where $Q_i$ and $Q_o$ are respectively the inlet and outlet gas flow, ml/min.

$CO_2$-loading $\alpha$. As shown in Fig. 3, the $CO_2$-loading in the unit volume lean/rich solution is measured by acidolysis overflow method. Each sample will be tested at least three times, and the average value and standard deviation will be analyzed (Eq. (6)).

$$\alpha = \frac{(V_2 - V_1)}{22.4 \times V_0 \times C} \times f \tag{6}$$

Where $\alpha$ is $CO_2$-loading of absorbents, mol $CO_2$/mol amine; $V_1$ and $V_2$ are respectively the $CO_2$ volume of pre/ post reaction, ml; $C$ is solution concentration, mol/L; $f$ is the temperature correction coefficient.

Enhancement factor $E$. The ratio of nanofluids' $CO_2$-loading volume to the blank solution's can be used to represent the $CO_2$ ab/desorption performance (Eqs. (7)-(8)):

$$E_{ab} = \frac{\partial_{ab}}{\partial_{ab-b}} \tag{7}$$

$$E_{de} = \frac{\partial_{de} - \partial_{de,eq}}{\partial_{de-b} - \partial_{de,eq-b}} \tag{8}$$

Where $E_{ab}$ and $E_{de}$ are the ab/desorption enhancement factors, respectively; $\alpha_{ab}$ and

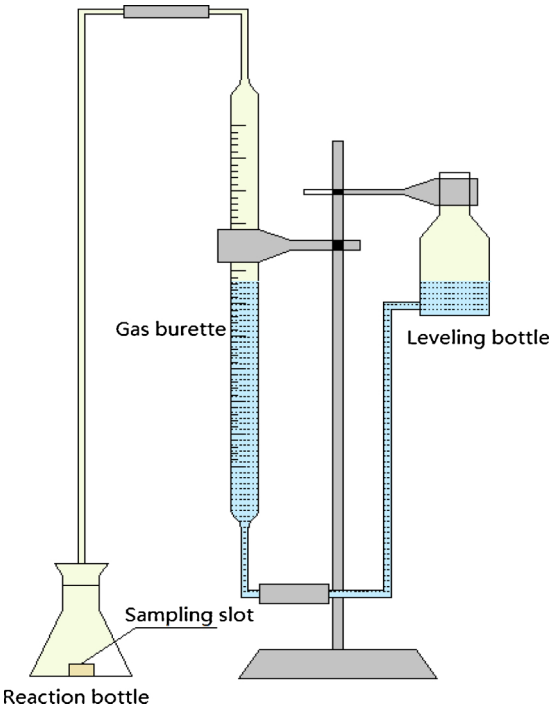


**Fig. 3.** Experimental diagram of acidolysis overflow method.

$\alpha_{ab,-b}$ are $CO_2$-loading of nanofluids and blank solution, respectively, mol $CO_2$/mol amine; $\alpha_{de}$, $\alpha_{de,eq}$, $\alpha_{de-b}$ and $\alpha_{de,eq-b}$ are the $CO_2$-loading of desorption process and reaction equilibrium state of nanofluids and blank solution.

Energy consumption. The energy consumption of the overall desorption process can be described as (Eqs. (9)-(10)):

$$Q_{de} = q_o - q_i \tag{9}$$

$$Q_{re} = \frac{Q_{de}}{(\partial_{de,rich} - \partial_{de,i}) \times C \times V_L} \quad (10)$$

Where $Q_{de}$ is the energy consumption of desorption process, KJ; $q_i$ and $q_o$ are the initial and final readings of electric power detector, respectively, MJ/kg $CO_2$. Where $Q_{re}$ is relative energy consumption of desorption process, $V_L$ is the volume of solution, L.

## 4. results and discussion

### 4.1. Amine solution concentration

Fig. 4 shows the effect of TETA mole fraction on $CO_2$ capture performance of $SiO_2$ nanofluids. It can be seen from Fig. 4 **a)** that the absorption rate keeps more than 890 ml/min at the beginning of the absorption process. When the reaction continues about 10–15 minutes, the absorption rate shows a downward trend, and eventually keep stable at lower than 40 ml/min. This indicates reactant TETA is constantly consumed during the $CO_2$ absorption process and eventually reaches equilibrium state. Fig. 4 **b)** indicates the vibration of desorption rate declines with time for nanofluids. The desorption process can be divided into three stages: Initial heating stage, the solution temperature rises to a near boiling state, during which the $CO_2$-loading decreases from the initial loading to the standard point. Primary regeneration stage, the solution remains in boiling state and most of the $CO_2$ is desorpted by heating. Post desorption stage, though the solution temperature remains at boiling point, the continuous heating can only regenerate small amount of $CO_2$.

It can also be found from Fig. 4 that both ab/desorption properties of nanofluids are better than those of blank solutions without nanoparticles. This indicates that the addition of nanoparticles can effectively promote the mass transfer performance, which is mainly due to the enhancement of liquid-phase turbulence and the Brown motion (Kim et al., 2007). For bubbling reactor, the rising process of bubbles will intensify the solution's liquid-phase turbulence and nanoparticles' macroscopic motion, thus the $CO_2$-loading of nanofluids promotes. In addition, Brownian motion is easier to cause the microscopic component mixing in liquid-phase interior; these perturbations to the boundary layer can promote the gas-liquid mass transfer capacity.

### 4.2. Ultrasonic vibration time

Fig. 5 shows the effect of ultrasonic vibration time on absorption rate. It can be found that the absorption rate grows with the increase of ultrasonic vibration time at the initial stage. However, when the ultrasonic vibration time last for more than 1.0 h, the absorption rate decreases. Furthermore, the absorption performance of nanofluids with ultrasonic vibration is better than the none-vibration conditions. Because ultrasonic vibration can make the nanoparticles follow directional movement, so that both the lateral and vertical distances remain relatively stable. Moreover, the ultrasonic vibration time also promote the Brownian movement of nanoparticles, which can improve the nanofluids' stability and enhance the mass transfer performance (Lee and Kang, 2013). When the time shortens, the vibration wave cannot influence the entire volume of nanofluids. The inadequate energy cannot sufficiently destroy the attraction between particles and prevent the settlement caused by particle aggregation. However, when the ultrasonic vibration time runs through the critical value, the superfluous internal energy will intensifies the possibility of bubbles' collision, which enables more nanoparticles to agglomerate and thus suppressed the mass transfer process.

### 4.3. Mass fraction of nanoparticle

Fig. 6. **a)** and **b)** shows the effect of nanoparticles' mass fraction on ab/desorption enhancement factor. With the growth of nanoparticle mass fraction, the nanofluids' ab/desorption performances respectively increase up to 1.29 and 1.23, and then diminishes. The reason is that the nanoparticles have a preferable $CO_2$ adsorption capacity, which can effectively enhance the $CO_2$ transport capacity in liquid film (Kars et al., 1979). When the nanoparticles' mass fraction keeps growing, the disturbance of gas-liquid interface and the effective surface area are promoted. Moreover, concentration gradient increase can facilitate the $CO_2$ transport capacity, the enlarged interface area also inhibits the bubbles' generation (Lee et al., 2011). However, when the nanoparticle mass fraction reaches a high value, a flat plate will be formed between the nanoparticles and block the path for rising bubbles (Karve and Juvekar, 1990). In this condition, the mass transfer performance weakens due to aggravated agglomeration and precipitation effect.

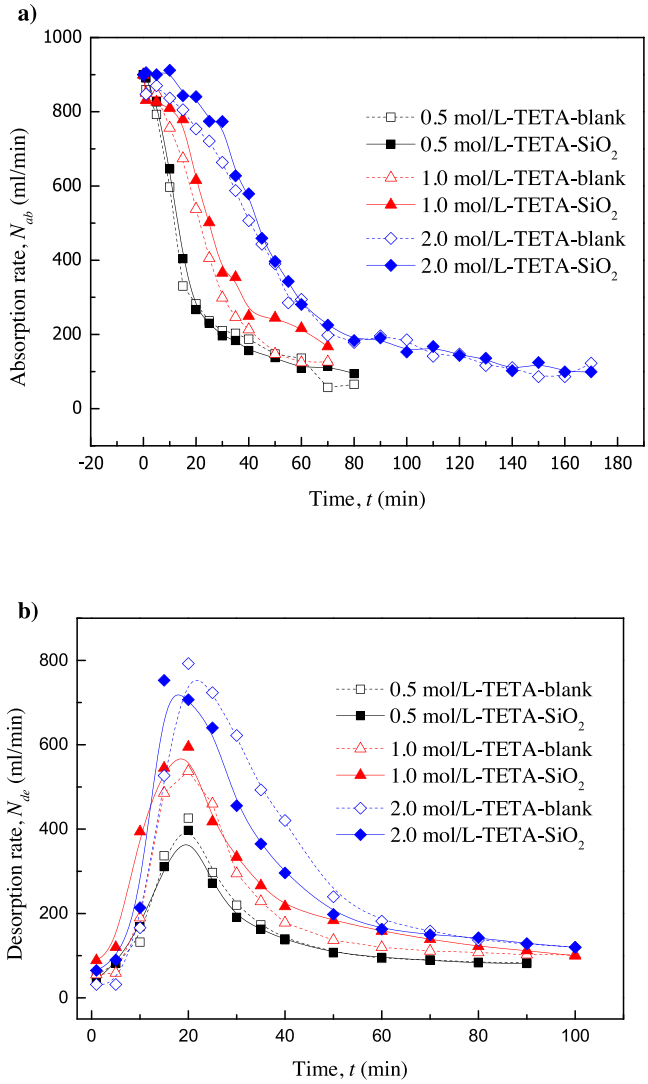


**Fig. 4.** Effect of TETA mole fraction on $CO_2$ capture performance of $SiO_2$ nanofluids. a) Effect of TETA mole fraction on absorption performance of $SiO_2$ nanofluids. b) Effect of TETA mole fraction on desorption performance of $SiO_2$ nanofluids.

### 4.4. Nanoparticle size

It can be seen from Fig. 7 **a)** that the $CO_2$-loading shows a growth trend with time during the absorption stage. The $CO_2$-loading increases rapidly at the beginning 0–30 min, and then keeps stable until the reaction reaches equilibrium. The curves' slope of ab/ desorption indicates that the nanofluids with higher particle size (45 nm) shows

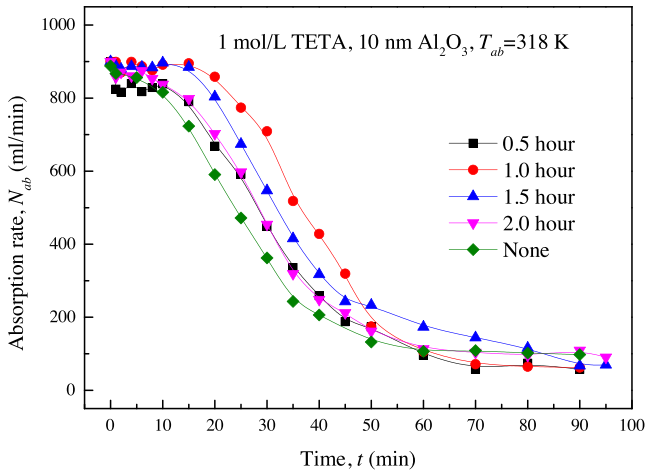


**Fig. 5.** Effect of ultrasonic vibration time on absorption rate.

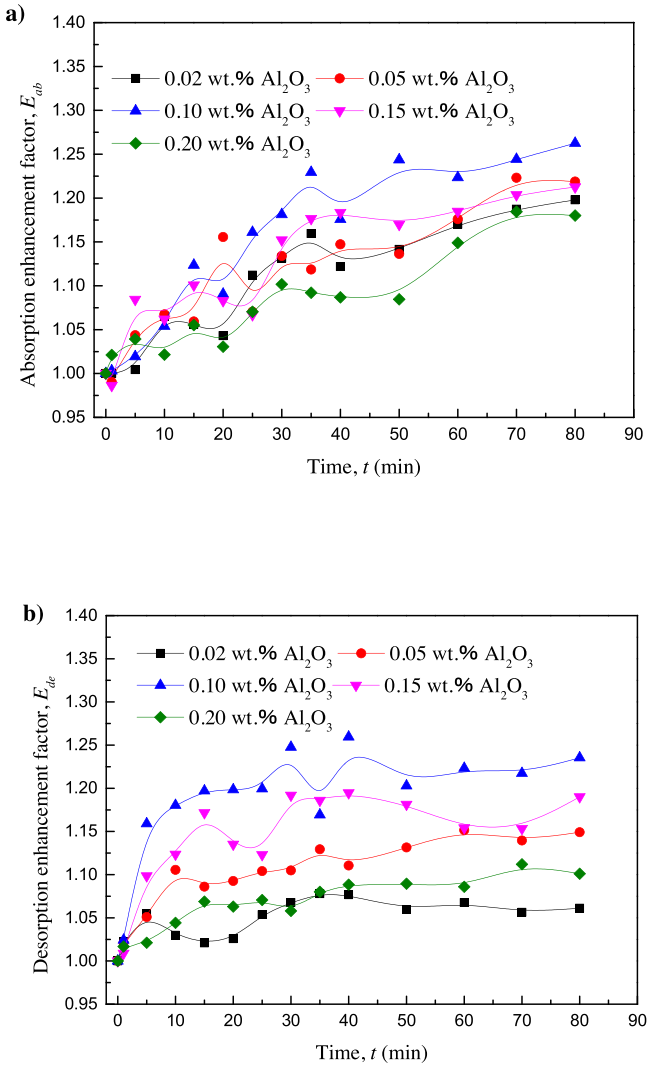


**Fig. 6.** Effect of nanoparticles' mass fraction on enhancement factor. a) Effect of nanoparticles' mass fraction on absorption enhancement factor. b) Effect of nanoparticles' mass fraction on desorption enhancement factor.

better mass transfer performance. This can be explained as follows: The shape of nanoparticles is considered as sphere, on which condition, the larger particle size can reduce the relative surface area and energy, the

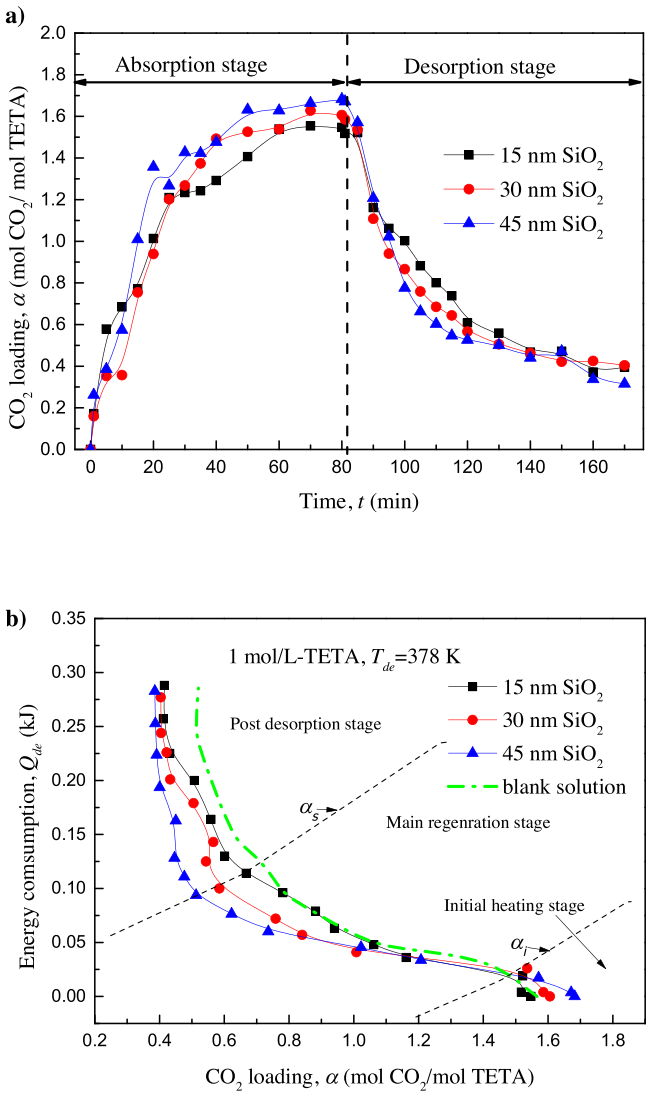


**Fig. 7.** Effect of nanoparticle size on $CO_2$ capture characteristics of nanofluids. a) Effect of nanoparticle size on $CO_2$-loading. b) Effect of nanoparticle size on energy consumption.

surface and quantum scale effects of nanoparticles weakens (Seyf and Nikaaein, 2012). Thus, the influence on the physical and chemical properties of nanofluids is insignificant due to its common characteristic. However, the agglomeration effect cannot be negligible, because the smaller particle size and the higher surface energy are more likely to cause agglomeration effect.

Fig. 7. **b)** shows the variation characteristics between $CO_2$ loading and energy consumption. In this figure, the desorption stages mentioned above can be more intuitively depicted, and the boundary $CO_2$-loading lines can be defined as initial and standard $CO_2$-loading ($\alpha_s$ and $\alpha_i$), respectively. With the decrease of $CO_2$-loading, the energy consumption slowly increase at high $\alpha$ value, and then sharply rises after reaches $\alpha_i$. The slow change of energy consumption indicates that a small external energy input can bring about significant $CO_2$ desorption in the main regeneration stage. On the contrary, the fast change of energy consumption shows that the absorbent has reached the post regeneration stage, which means the continued energy addition cannot evidently promote the desorption effect. Besides that, the 45 nm $SiO_2$ showed lower energy consumption compared with the others when the $CO_2$-loading reaches $\alpha_s$. This also proves that the larger nanoparticles have better $CO_2$ desorption performance.

It can also be found in Fig. 7. **b)** that the nanofluids shows lower

**Table 3**
Thermal parameters of $SiO_2$ nanofluids and blank solution.

| Temperature | Subject | | Blank solution | 15 nm $SiO_2$ | 30 nm $SiO_2$ | 45 nm $SiO_2$ |
|---|---|---|---|---|---|---|
| 293.15 K | Thermal conductivity | (W/(m· K)) | 0.494 | 0.505 | 0.512 | 0.517 |
| | Thermal diffusivity | ($mm^2$/s) | 0.129 | 0.131 | 0.135 | 0.144 |
| | Specific heat | ($MJ/m^{8}$· K) | 3.866 | 3.851 | 3.785 | 3.665 |
| 363.15 K | Thermal conductivity | (W/(m· K)) | 0.657 | 0.690 | 0.705 | 0.713 |
| | Thermal diffusivity | ($mm^2$/s) | 0.191 | 0.235 | 0.245 | 0.249 |
| | Specific heat | ($MJ/m^{8}$· K) | 3.429 | 2.934 | 2.886 | 2.867 |

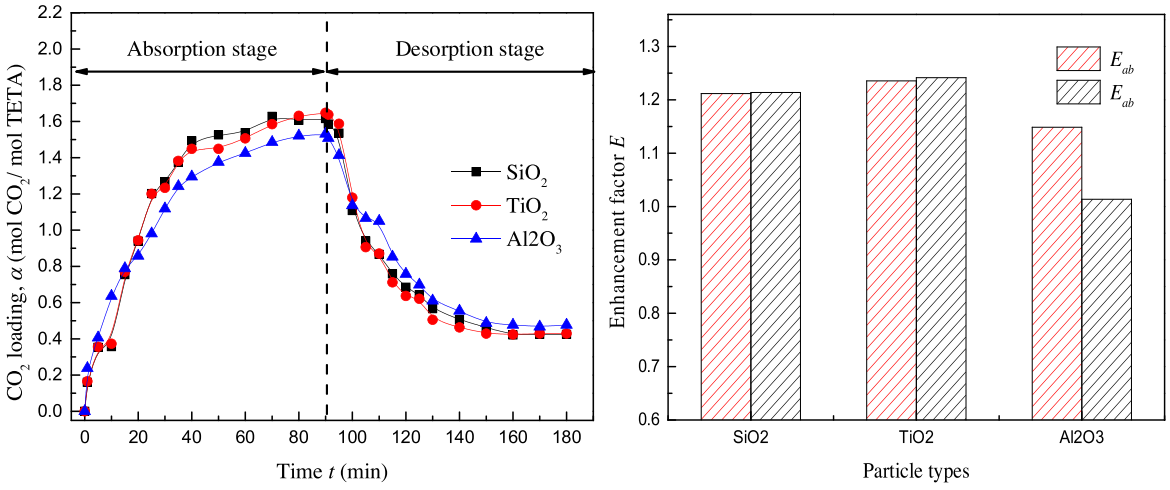


**Fig. 8.** Effect of Nanoparticle types on ab/desorption performance.

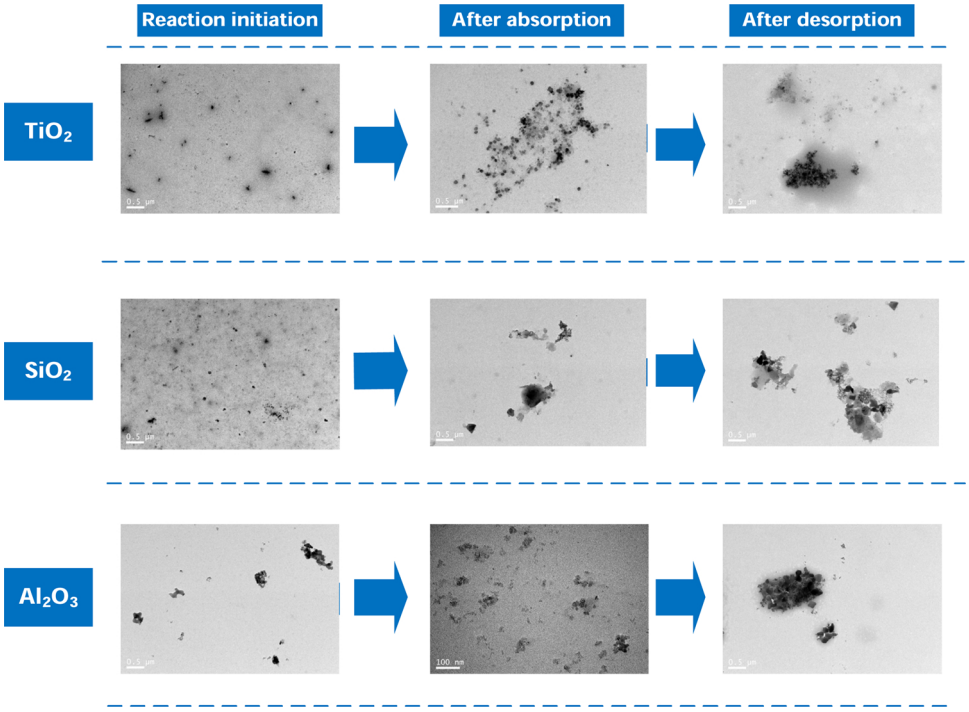


**Fig. 9.** TEM image of different type of nanoparticles ($TiO_2$, $SiO_2$ and $Al_2O_3$) before and after ab/desorption processes.

energy consumption than blank TETA solutions, which is because higher heat flux would make more heat distributed to the $CO_2$ desorption by the addition of nanoparticles, and thermal parameters tested and shown in Table 3 further evidence it. The thermal conductivity of nanofluids is higher than blank solution, especially at high temperature. The reason can be explained as follows: The nanoparticles themselves applied in this work have a lower thermal conductivity, the strengthening heat transfer is mainly realized by the nanoparticles' Brown motion. When the temperature grows higher, the microscopic motion becomes intense, thus promoting the heat transfer process, which is proved by the fact that the addition of nanoparticles demonstrates a more considerable improvement of thermal conductivity at 363 K.

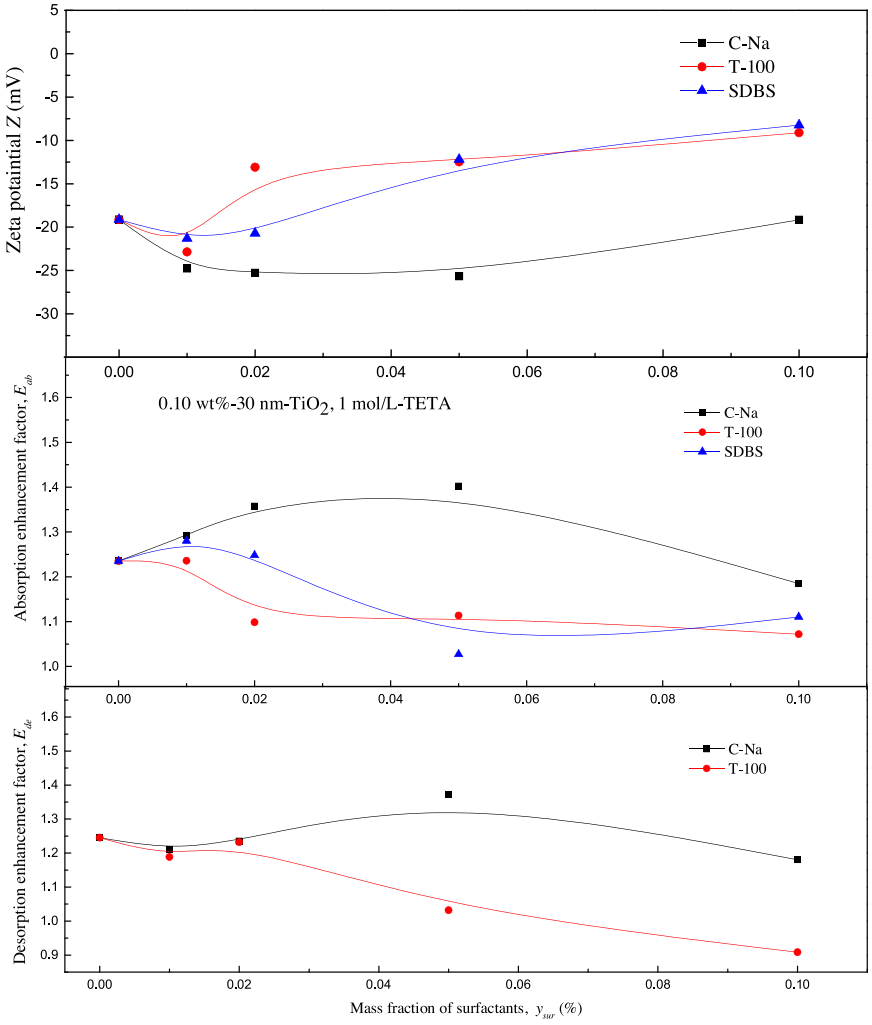


**Fig. 10.** Addition of surfactant influences the $CO_2$ capture performances in nanofluids.

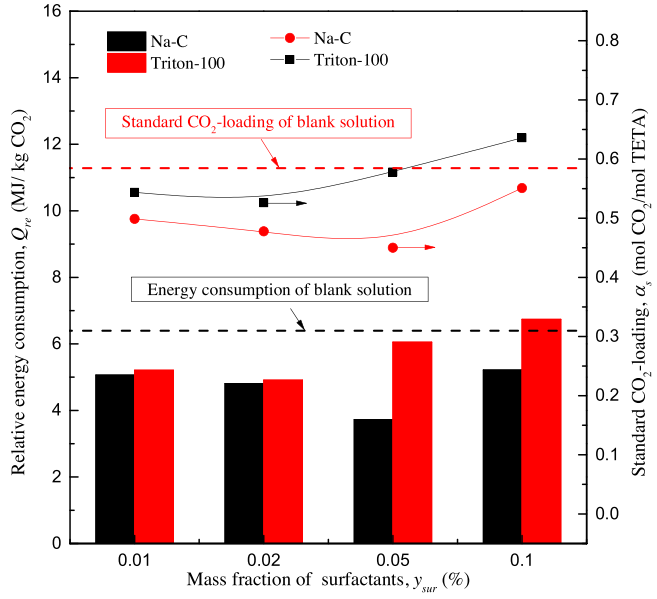


**Fig. 11.** Effect of surfactants' mass fraction on desorption energy of nanofluids.

### 4.5. Nanoparticle types

In order to investigate the effect of different nanoparticle types on ab/desorption performance, $SiO_2$, $Al_2O_3$ and $TiO_2$ particles with the same size of 30 nm were adopted in this study. It can be seen from Fig. 8 that the enhancement factors of both ab/desorption for $TiO_2$ and $SiO_2$ are very close and evidently higher than $Al_2O_3$, the sequence is similar to Wang's work (Wang et al., 2016). The reason is that Ti and Si are congeners of the elements, the properties of their oxides are similar. Jiang's study (Jiang et al., 2014) proved that the mass transfer performance of nanofluids was strengthened by the $CO_2$ adsorption performance of nanoparticles. The $TiO_2$ and $SiO_2$ have higher $CO_2$ adsorption affinity than $Al_2O_3$, which makes it easier for $CO_2$ to be absorbed into gas-liquid interface and accelerate the ab/desorption reaction.

Fig. 9 illustrates the TEM image of different type of nanoparticles ($TiO_2$, $SiO_2$ and $Al_2O_3$) before and after ab/desorption processes. It can be seen that that the nanoparticles exhibit excellent dispersibility after being shattered by ultrasonic dispersion. After absorption, agglomeration effect begin to occur in nanofluids, a small amount of organic substance surround the nanoparticles. And the diameter of particle clusters continually increases during desorption process. The result indicates that the dispersibility of nanoparticles deteriorates as the ab/desorption reaction was prolonged. The agglomerated clusters hinder the Brownian motion and raise the mass transfer residence of nanofluids, which will increase the residence time of $CO_2$ at gas-liquid

interface and weaken the mass transfer performance.

### 4.6. Mass fraction of surfactants

It can be seen from Fig. 10 that the addition of surfactant influences the $CO_2$ capture performances in nanofluids. The enhancement factor increases with the growth of mass fraction of C-Na, and the maximum value occurred at 0.05 wt.% C-Na. And the nanofluids' zeta potential keeps below -19.14 mV, which indicates that the electrostatic repulsion force between particles is dominant and the nanoparticles are well dispersed. This is because the addition of C-Na can stimulate dissociation in the liquid matrix, which promotes the ionized ions to get charged and adsorb on the nanoparticles' surface to form electric potential, which will prevent the same charged particles from approaching and enhance the stability of nanofluids with longer retention time. Besides that, C-Na is a salt of strong base and weak acid showing alkalinity after hydrolysis, and the salt itself has a certain $CO_2$ adsorption capacity, which can also promotes the mass transfer process (Maji and Chakraborty, 2018).

However, the $y_{sur}$ growing of Triton X-100 and SDBS shows fair $CO_2$ capture performance. The addition of both surfactants leads to zeta potential' rising, which means that the Van der Waals force between nanoparticles is dominant and the agglomeration effect is intensified, the desperation performance become unstable. As for Triton X-100, the $E_{ab}$ shows a tiny promotion at 0.01 wt.% and then declines, the $E_{de}$ shows a trend of single reduction with $y_{sur}$ increase. The reason can be explained as follows: Triton X-100 is a nonionic surfactant, which exists in amine-solvent as the molecule form, a water-made film can wrap its surface due to the hydrophilicity effect (Choi et al., 2018). Such effect can enhance the performance of steric stabilization and promote the mass transfer capacity. However, when the mass fraction of Triton X-100 reached a high value, the amount of free Triton X-100 molecules increases. The lipophilic group of free surfactants bounds to the hydrophilic group on the surface of the nanoparticles, which can eventually lead to suspension instability.

Moreover, small amount of SDBS can enhance the mass transfer performance due to the electric barrier, which makes the nanoparticles dispersed more evenly in the liquid phase (Yan et al., 2012). However, restraint action of mass transfer process appears when $y_{sur}$ of SDBS exceeds 0.01 wt.%. On one hand, a superfluous SDBS brings about supersaturated adsorption and form overabundant long chains of cross-linking macromolecule. On the other hand, SDBS strengthens mechanical strength of bubble so that intensifies the foaming behavior. Especially for desorption stage, the foaming effect not only block the $CO_2$ transfer, but also generate acute amplitude of system pressure. Therefore, SDBS is not recommended for the preparation of amine-based nanofluids.

Fig. 11 shows the effect of surfactants' mass fraction on desorption energy of nanofluids. The $\alpha_s$ of Triton X-100 has a monotone increasing trend. Especially at 0.10 wt.%, the main $\alpha s$ value outnumbers the blank $CO_2$-loading line, which suggests that the inhibition effect drastically influences the $CO_2$ desorption process in this time. Moreover, the $\alpha_s$ of C-Na grows after an initial decline, and the $\alpha_s$ under all conditions are below the standard $CO_2$-loading line of blank solution, which proves the C-Na nanofluids have preferable mass transfer performance. In particular, the minimum $\alpha_s$ attains 0.47, which indicates that C-Na nanofluids can realize deeper-level desorption. Furthermore, it can also be seen from Fig. 11 that the energy consumption of C-Na nanofluids keeps a low level at 0.01-0.1 wt.%, the lowest energy consumption is 40.41% less than blank solution's. This because the $CO_2$-loading difference of C-Na nanofluids is much higher than blank solution for the cases with a little difference of energy intake. Moreover, the energy consumption principles of Triton X-100 is similar with $E_{de}$ and $\alpha_s$ as shown previously.

## 5. Conclusion

In this study, a bubbling reaction system was implemented to comprehensively study the $CO_2$ capture properties of TETA-based nanofluids. Three kinds of nanoparticles and surfactants were adopted to develop nanofluids in this study. The vital parameters, such as ultrasonic vibration time, particle size and surfactants mass fraction, were considered to determine the performance of ab/desorption rate, $CO_2$-loading, energy consumption, etc.

- Nanofluids shows better $CO_2$ capture performance than blank TETA solutions, which is mainly due to the enhancement of liquid-phase turbulence and the Brown motion of nanoparticles.
- 1 h is considered as the most reasonable ultrasonic time for $CO_2$ absorption performance of nanofluids in this experimentation.
- There exist an optimal $SiO_2$-nanoparticle mass fraction of 0.10 wt.%, the enhancement factors $E_{ab}$ and $E_{de}$ can respectively increase to 1.29 and 1.23.
- The larger particle size can reduce the relative surface area and energy. The 45 nm $SiO_2$ shows lower energy consumption when the $CO_2$-loading reaches $\alpha_s$.
- Enhancement factors of both ab/desorption for $TiO_2$ and $SiO_2$ are very close and evidently higher than $Al_2O_3$ due to the nanoparticles' different $CO_2$ adsorption performance.
- The addition of surfactants can effectively promote the mass transfer performance of nanofluids, but Triton X-100 and SDBS can cause the inhibition effect when mass fraction exceeds 0.01 wt.%.

## Declarations of interest

None.

## Acknowledgement

This work was funded by the National Key Research and Development Program of China (Grant 2017YFB0603403).

## References

Abu-Zahra, M.R.M., Niederer, J.P.M., Feron, P.H.M., Versteeg, G.F., 2007. CO 2 capture from power plants. Int. J. Greenh. Gas Control. 1, 135–142.
Chen, C., Wang, Z., Wei, W., Cheng, C., Wang, J., Zhou, J., Che, Y., 2011. Research of carbon dioxide absorption and desorption in organic amine aqueous solutions. China Environ. Sci. 31, 1109–1114.
Choi, S.U.S., 1995. Enhancing thermal conductivity of fluids with nano-particles. Asme Fed 231, 99–105.
Choi, T.J., Jang, S.P., Kedzierski, M.A., 2018. Effect of surfactants on the stability and solar thermal absorption characteristics of water-based nanofluids with multi-walled carbon nanotubes. Int. J. Heat Mass Transf. 122, 483–490.
Eastman, J.A., Choi, U.S., Li, S., Thompson, L.J., Lee, S., 1996. Enhanced thermal conductivity through the development of nanofluids. Mrs Proceedings. pp. 457.
Fang, M., Wang, Z., Yan, S., Cen, Q., Luo, Z., 2012. $CO_2$ desorption from rich alkanolamine solution by using membrane vacuum regeneration technology. Int. J. Greenh. Gas Control. 9, 507–521.
Goto, K., Yogo, K., Higashii, T., 2013. A review of efficiency penalty in a coal-fired power plant with post-combustion $CO_2$ capture. Appl. Energy 111, 710–720.
Jiang, J., Zhao, B., Zhuo, Y., Wang, S., 2014. Experimental study of CO 2 absorption in aqueous MEA and MDEA solutions enhanced by nanoparticles. Int. J. Greenh. Gas Control. 29, 135–141.
Jilvero, H., Normann, F., Andersson, K., Johnsson, F., 2012. Heat requirement for regeneration of aqueous ammonia in post-combustion carbon dioxide capture. Int. J. Greenh. Gas Control. 11, 181–187.
Kars, R.L., Best, R.J., Drinkenburg, A.A.H., 1979. The sorption of propane in slurries of active carbon in water. Chem. Eng. J. 17, 201–210.
Karve, S., Juvekar, V.A., 1990. Gas absorption into slurries containing fine catalyst particles. Chem. Eng. Sci. 45, 587–594.
Kim, J.-K., Jung, J.Y., Kang, Y.T., 2006. The effect of nano-particles on the bubble absorption performance in a binary nanofluid. Int. J. Refrig. 29, 22–29.
Kim, J.-K., Jung, J.Y., Kang, Y.T., 2007. Absorption performance enhancement by nano-particles and chemical surfactants in binary nanofluids. Int. J. Refrig. 30, 50–57.
Kim, Y.E., Moon, S.J., Yoon, Y.I., Jeong, S.K., Park, K.T., Bae, S.T., Nam, S.C., 2014. Heat of absorption and absorption capacity of $CO_2$ in aqueous solutions of amine containing multiple amino groups. Sep. Purif. Technol. 122, 112–118.
Kong, Z., Dong, X., Liu, G., 2016. Coal-based synthetic natural gas vs. Imported natural

gas in China: a net energy perspective. J. Clean. Prod. 131, 690–701.
Lee, J.W., Jung, J.-Y., Lee, S.-G., Kang, Y.T., 2011. $CO_2$ bubble absorption enhancement in methanol-based nanofluids. Int. J. Refrig. 34, 1727–1733.
Lee, J.W., Kang, Y.T., 2013. $CO_2$ absorption enhancement by $Al_2O_3$ nanoparticles in NaCl aqueous solution. Energy 53, 206–211.
Liu, H., Gallagher, K.S., 2010. Catalyzing strategic transformation to a low-carbon economy: a CCS roadmap for China. Energy Policy 38, 59–74.
Liu, S., Gao, H., He, C., Liang, Z., 2019a. Experimental evaluation of highly efficient primary and secondary amines with lower energy by a novel method for post-combustion $CO_2$ capture. Appl. Energy 233-234, 443–452.
Liu, S., Gao, H., Luo, X., Liang, Z., 2019b. Kinetics and new mechanism study of $CO_2$ absorption into water and tertiary amine solutions by stopped-Flow technique. AIChE J. 65, 652–661.
Maji, N.C., Chakraborty, J., 2018. Low-cost and high-throughput synthesis of copper nanopowder for nanofluid applications. Chem. Eng. J. 353, 34–45.
Moraveji, M.K., Golkaram, M., Davarnejad, R., 2013. Effect of CuO nanoparticle on dissolution of methane in water. J. Mol. Liq. 180, 45–50.
Nagy, E., Feczkó, T., Koroknai, B., 2007. Enhancement of oxygen mass transfer rate in the presence of nanosized particles. Chem. Eng. Sci. 62, 7391–7398.
Notz, R., Mangalapally, H.P., Hasse, H., 2012. Post combustion $CO_2$ capture by reactive absorption: pilot plant description and results of systematic studies with MEA. Int. J. Greenh. Gas Control. 6, 84–112.
Pohlmann, J., Bram, M., Wilkner, K., Brinkmann, T., 2016. Pilot scale separation of CO 2 from power plant flue gases by membrane technology. Int. J. Greenh. Gas Control. 53, 56–64.
Roizard, C., Poncin, S., Lapicque, F., Py, X., Midoux, N., 1999. Behavior of fine particles in the vicinity of a gas bubble in a stagnant and a moving fluid. Chem. Eng. Sci. 54, 2317–2323.
Ruthiya, K.C., Kuster, B.F.M., Schouten, J.C., 2010. Gas-liquid mass transfer enhancement in a surface aeration stirred slurry reactors. Can. J. Chem. Eng. 81, 632–639.
Saiwan, C., Chanchey, A., Supap, T., Idem, R., Tontiwachwuthikul, P., 2013. Ammonia emission kinetics of monoethanolamine (MEA) based $CO_2$ absorption process. Int. J. Greenh. Gas Control. 12, 333–340.
Schäffer, A., Brechtel, K., Scheffknecht, G., 2012. Comparative study on differently concentrated aqueous solutions of MEA and TETA for $CO_2$ capture from flue gases. Fuel 101, 148–153.
Sema, T., Naami, A., Fu, K., Edali, M., Liu, H., Shi, H., Liang, Z., Idem, R., Tontiwachwuthikul, P., 2012. Comprehensive mass transfer and reaction kinetics studies of $CO_2$ absorption into aqueous solutions of blended MDEA–MEA. Chem. Eng. J. 209, 501–512.
Seyf, H.R., Nikaaein, B., 2012. Analysis of Brownian motion and particle size effects on the thermal behavior and cooling performance of microchannel heat sinks. Int. J. Therm. Sci. 58, 36–44.
Sharma, M.M., 1965. Kinetics of reactions of carbonyl sulphide and carbon dioxide with amines and catalysis by Brönsted bases of the hydrolysis of COS. Transactions of the Faraday Society 61, 681–688.
Wang, T., Yu, W., Liu, F., Fang, M., Farooq, M., Luo, Z., 2016. Enhanced $CO_2$Absorption and Desorption by Monoethanolamine (MEA)-Based Nanoparticle Suspensions. Ind. Eng. Chem. Res. 55, 7830–7838.
Wang, Z., Fang, M., Pan, Y., Yan, S., Luo, Z., 2013. Comparison and selection of amine-based absorbents in membrane vacuum regeneration process for $CO_2$ capture with low energy cost. Energy Procedia 37, 1085–1092.
Wang, Z., Liu, T., 2015. Scenario analysis of regional carbon reduction targets in China: a case study of Beijing. J. Renew. Sustain. Energy 7, 043125.
Xie, W., Zhang, J., Xu, L., Lv, J., Zhong, H., Sheng, C., 2017. Influence of particles on mass transfer performance for $CO_2$ absorption using K2CO3 solution in a random θ-ring packed column. Int. J. Greenh. Gas Control. 58, 81–86.
Yan, H.C., Li, Q.X., Geng, T., Jiang, Y.J., 2012. Properties of the quaternary ammonium salts with novel counterions. J. Surfactants Deterg. 15, 593–599.
Yuan, M., Gao, G., Hu, X., Luo, X., Huang, Y., Jin, B., Liang, Z., 2018. Premodified sepiolite functionalized with Triethylenetetramine as an effective and inexpensive adsorbent for $CO_2$ capture. Ind. Eng. Chem. Res. 57, 6189–6200.
Zhang, Y., Zhao, B., Jiang, J., Zhuo, Y., Wang, S., 2016. The use of $TiO_2$ nanoparticles to enhance $CO_2$ absorption. Int. J. Greenh. Gas Control. 50, 49–56.